In Vivo Lumbar Intervertebral Disc Deformation During Lateral Bending Motion Under Different Load-Bearing Conditions

Haoxiang Xu
Tianjin Medical University
Wangqiang Wen
Tianjin Medical University
Zepei Zhang
Tianjin Hospital
Bowen Kou
Tianjin Medical University
Jincheng Wu
Tianjin Medical University
Hanpeng Xu
Tianjin Medical University
Jun Miao (mj6688@163.com)
Tianjin Hospital https://orcid.org/0000-0001-6689-4316

Research

Keywords: Intervertebral disc, in-vivo kinematics, Lower lumbar spine, weightbearing, disc deformation, Fluoroscope, Lateral bending

DOI: https://doi.org/10.21203/rs.3.rs-423428/v1

Abstract

Background

Lumbar Intervertebral Disc Degeneration (LDD) is one of the largest health worldwide problems, based on lost working time and associated costs. Inappropriate mechanical loading is considered to be an important factor in the development of LDD. L3-4 and L4-L5 were the commonly affected levels. Recent studies have measured geometric deformation of lumbar intervertebral discs during an in vivo functional weightbearing of the lumbar. The purpose of the present study was to determine the lumbar disc deformation in living human subjects during lateral bending motion under different load-bearing conditions.

Methods

11 healthy subjects, 6 males and 5 females, aged 21 ≤ 39 years, with an average age of 30 ± 5 years, were recruited for the present study. Using the combination of dual fluoroscopic imaging system(DFIS)and CT, the sagittal images of L3-5 segments scanned by CT were transformed into three-dimensional reconstruction models and then matched to the instantaneous images of lumbar spine motion taken by a double fluorescent X-ray system under different loads. Motions were reproduced with the use of the combined imaging technique during left and right bending movements. Then, the kinematics data of the height, tension and compression deformation, and shear deformation of the lumbar intervertebral disc were obtained by using computer-related software.

Result

The data indicated that the tendency of tensile deformation during left and right bending was approximately symmetric. During the functional bending of the body, there was a greater compression deformation behind the same side of the movement and a higher tension deformation in front of the contralateral movement. The magnitude changed along the diagonal towards the posterolateral direction. During left bending, the upper vertebrae had a larger deformation range and tension deformation than the lower vertebrae. Meanwhile, it was not found that the small load had a significant effect on the tensile deformation of the intervertebral disc.

Conclusion

Lumbar disc deformation showed direction-specific and level-specific changes during lateral bending motion. These results could help understand the physiological motion characters of the lumbar spine and provide data support for other biomechanical studies.

Introduction

Spine-related pain and dysfunction are believed to be initiated by intervertebral disc degeneration. The development and progression of intervertebral disc degeneration are influenced by the complex interactions between cells, extracellular matrix, and mechanical loading. Accurate mechanical characterization of the IVD is instrumental for understanding the mechanisms of IVD related spinal physiopathology and for helping to improve surgical treatments of lumbar disease such as prosthetic intervertebral discs.

Due to the complicated spinal anatomy and physiological loading conditions of the spine, it has been a challenge in the past to determine the in-vivo deformation of the IVD. Numerous studies have aimed to examine the lumbar complex structures and biomechanical behavior of the lumbar discs using both in vitro and in vivo approaches.[1–13]For example, sagittal magnetic resonance (MR) has been used to study the height of different disc components in the non-weight-bearing supine position, and to compare the segmental dependence.[14] In vivo motion of the lumbar spine has often been evaluated by using three-dimensional (3D) fluoroscopic imaging and CT or MRI. Cadaveric studies measured lumbar segment kinematics by applying six degrees of freedom (6DOF) using various mechanical loading equipment setups, with or without a compressive load.[3, 10, 12, 13, 15–17] Finite element (FE) models have been developed to study lumbar disc deformation under various simulated loading conditions.[5, 18] However, these only focused on the static anatomical characteristics or in vitro motion parameters. Recently, some researchers used a combined dual fluoroscopic imaging system (DFIS) and the MR imaging technique to investigate the dynamic flexion motion of intervertebral segments of the lumbar spine and observe different motion patterns among the lumbar intervertebral segments. Wang et al. investigated motion characteristics of lumbar segments in vivo and measured the geometric deformation of lumbar intervertebral discs under in-vivo weightbearing conditions during standing. [19, 20]

However, to the best of our knowledge, few studies have been reported to investigate the in-vivo lumbar intervertebral disc deformation under different load-bearing conditions and various motion states. The purpose of this study is to investigate In vivo lumbar intervertebral disc deformation during lateral bending motion under different load-bearing conditions. We hypothesized that the intervertebral segment deformation of the lumbar spine is segmental level-dependent.

Material And Methods

Patient recruitment

Eleven healthy subjects, 6 males and 5 females, aged 21≤39 years, with an average age of 30±5 years, were recruited for the present study. None of the lumbar specimens had previous spinal surgery. We also excluded the specimens with bridging osteophytes, obvious osteoporosis, and other severe lumbar degenerative diseases as determined by CT images read by a senior radiologist. The study protocol was approved by the author’s Internal Review Board（IRB）. All patients provided written informed consent.

Lumbar disc deformations at the L3-4 and L4-5 segments of each subject were investigated; thus, a total of 22 discs were studied.

Three-dimensional vertebral models

All subjects were CT (Sensation 16, Siemens AG, Germany) scanned in supine positions. Parallel digital images of the lumbar spine with a thickness of 0.625 mm, no gap, and a resolution of 512×512 pixels were obtained. Three-dimensional models of the L3-5 vertebrae were constructed using the 3D CT images in solid modeling software (Mimics 19.0 Materialise's Interactive Medical Image Control System□ Belgium). A cartesian coordinate system was created independently for each vertebral body□L3~5□using endplate plane and vertebral symmetry to describe the vertebral kinematics. The x-y plane was parallel to the upper endplate surface. The x-axis was defined in the left and the y-axis posterior directions of the vertebral body. The z-axis is perpendicular to the x-y plane and is pointing proximally [9,21] (Fig. 1a).

Dual fluoroscopic imaging

The lumbar spine of each subject during lateral bending motion (carrying 5kg sandbags front and back) was imaged using a dual fluoroscopic imaging system (DFIS) consisting of two fluoroscopes (BV Pulseras; Phillips, Bothell, WA) with their intensifiers orthogonal positioned perpendicular to each other. The subject performed the activity by bending the body from a standing position to the maximal position (Fig. 1b). Another researcher immobilized the subject's pelvis and buttocks and the standing posture and motor pattern were carefully guided to maintain accuracy. The two orthogonal fluoroscopic images had a resolution of 1024×1024 pixels with pixel size 0.3×0.3 mm^2.

Reproduction of in-vivo spine kinematics

A virtual DFIS environment was rebuilt in Rhinoceros (version 5.0, Robert McNeel & Associates, United States) to mimic the experimental setup according to the actual positions of two fluoroscopes. Then the pairs of fluoroscopic images were imported into the software environment. 3-dimensional models of L3~5 created from CT images were imported into the DFIS environment to create virtual projection images. The in-vivo 3D vertebral positions were reproduced when each virtual projection image of the models best matched independently X-ray imagine by translation and rotation in DFIS (Fig. 2). The overall accuracy and repeatability of this system have been validated for the determination of vertebral positions in space using a series of experiments [19,22,23].

Measurements and Statistical analysis

The intervertebral disc shape was constructed through the 3D volume between the adjacent upper and lower endplates. Deformation of the intervertebral disc was calculated using evenly distributed mesh vertices on the upper and lower endplates (approximately 3000 points per surface). The coordinate system of the upper endplate surface of the lower vertebra was used as a reference for the calculation of displacement of each corresponding point of the lower endplate of the upper vertebra to describe the intervertebral disc deformation. The non-weightbearing, supine position during CT scan was used as a reference to calculate the Shear and compression deformation of each point of the intervertebral disc during lateral bending motion under different load-bearing conditions. The overall compression deformation was measured in the proximal-distal direction (z-axis direction) in the reference coordinate system and plotted on a heat map. Shear deformation was obtained using the projection of the elongation in the x y plane of the reference coordinate system.

General distributions of shear and compression deformation were analyzed from the average of all subjects. The magnitude of shear and compression deformations were also quantitatively examined at 9 representative locations on the surfaces of the discs: left-anterior, anterior, right-anterior, left, center, right, left-posterior, posterior, right-posterior points of each disc to represent the deformational characteristics of different regions of the disc (Fig. 1c).

A two-factor analysis of variance was used to compare the differences of disc（L2-3, L3-4）shear ,and tensile deformation during lateral bending motion under different load-bearing conditions of the different vertebral levels. Statistical significance was set at $p < 0.05$. Statistical analysis was performed with the SPSS 20.0 software (IBM Corp., Armonk, New York).

Results

1. Disc deformation distribution

Going from the CT supine (non-weightbearing) to the left bending (weightbearing) positions, the right-anterior quarter of the L3-4 disc was in tension (+) while the left-posterior three quarters was in compression (-) (Fig. 3). The magnitude changed along the right-anterior to left-posterior direction from +11% to -37%. The L3-4 disc with load (10kg) had a similar conversion from 8% to -36%. For the L4-5 disc (weightbearing), the overall portion was under compression which gradually increases in compression along the right anterior to left posterior direction from +2% to -32%. Meanwhile, the L4-5 disc with load (10kg) had a similar conversion from 8% to -36%.

Besides, during the right bending (weightbearing), the left-anterior quarter of the L3-4 disc is in a stretched state (+), and the right-posterior 3/4 disc is in a compressed state (-). The trend changes along the diagonal, from +8% to -30%. The L3-4 disc has a similar transformation under the 10kg load condition; however, the trend direction is more toward the midline. For L4-5 discs, only the left anterior one-fifth of the disc is in a tension state (+) under weightbearing, and almost the entire L4-5 intervertebral discs are in a compressed state under a 10kg load (from the left-anterior side -39% to the right-posterior side 0 %).

2. Disc deformation at discrete locations

The tensile and shear deformations were quantitatively described at the 9 representative locations and plotted (Fig. 4 and 5). The tensile deformations at the L3-4 and L4-5 discs had similar trends. But the range of tensile deformation (difference between maximum tension and maximum compression) of L3-4 discs (35%) was significantly greater than that of L4-5 discs (22%) (P = 0.012) during left bending movement. During the left bending, the L3-4 showed maximal tensile deformations at the right-anterior location, both of which were +8% under weightbearing and 10kg loading, compared with +2% (weightbearing) and +1% (10kg loading) of the L4-5 (P =0.006). The deformation of the L3-4 and L4-5 discs decreased along diagonal towards the left-posterior direction, and acquired maximum compressive deformation at the left-posterior locations, - 27% and - 21% (P = 0.56) under weightbearing, - 25% and - 20% under 10 kg weightbearing (P = 0.09). Different from the compressive deformation of L4-5, the L3-4 showed tensile deformation under weightbearing and 10kg load on the anterior location (P = 0.035) and the right location (P = 0.085).

The tendency of tensile deformation during left and right bending was approximately symmetric (Fig. 4). The maximum tensile deformation of L3-4 and L4-5 discs were obtained in the left-anterior location, which was +6% and 4% under weightbearing, and +5% and +2% under 10kg load (p=0.35). Symmetrically, the deformation decreases along the diagonal of the disc to the right-posterior direction, and the deformation of the right-posterior region is almost compression deformation. The maximum compression deformations of L3-4 and L4-5 discs in the left-posterior portion were - 22% and -23% under weightbearing, but - 22% and - 20% under 10kg loading.

The magnitudes of shear deformation on the L3-4 and L4-5 discs at 9 locations were rather constant (Fig. 5). On average, the shear deformations ranged from 30% to 60%. There was no significant difference in the shear deformations between different load-bearing conditions. However, during right-bending movement, the deformation of L3-4 discs was significantly greater than that of the L4-5 (P = 0.044) at anterior locations.

Discussion

Quantitative data on vertebral body movement in the body is essential to enhance our understanding of spinal pathology and improve the current surgical treatment of spinal diseases. As the most basic exercise mode, side bending exercise participates in the formation of daily movements, but it is rarely studied separately. At the same time, few studies have investigated the influence of different weights on changes in exercise patterns. In this study, we investigated the lumbar vertebral disc deformation in asymptomatic living subjects when they performed standardized lateral bending under different load-bearing conditions. In general, the measured tensile deformation of the L3-4 and L4-5 discs is very small, ranging from 15% to -40%, and the shear strain range is rather constant from 30–60%. The data demonstrated that during left bending, the upper intervertebral disc (L3-4) had larger ranges of deformation than the lower intervertebral disc (L4-5). The tendency of tensile deformation during left and right bending was approximately symmetric. During the functional bending of the body, there is a greater compression deformation behind the same side of the movement and a higher tension deformation in front of the contralateral movement. Meanwhile, it was not found that the small load had a significant effect on the tensile deformation of the intervertebral disc.

Many studies have investigated the biomechanics of the lumbar spine, including those that described the morphological features of human lumbar discs and examined the range of motion or biomechanical responses of the lumbar spine to external loads. Zhong et al. [14] Obtained in vivo morphological features of human lumbar discs according to Magnetic resonance images of the lumbar spine of 41 young Chinese. The data showed segment-dependent geometric features of the lumbar IVD. Notably, the disc height and length of L4-5 are significantly larger than the upper lumbar disc. In vitro cadaveric tests have examined the biomechanical responses of the disc to external loads using various mechanical loading equipment setups. Fu et al. [13] measured the segment-dependent changes in lumbar intervertebral space height during flexion-extension motion in a custom-made mechanical loading equipment set-up. The author found that the changes in disc height at L4/5 were different from those at the L3/4 during flexion-extension motion. The changes in anterior and posterior disc heights were similar at the L4/5 level from neutral to extension, but the changes in anterior disc height were significantly greater than those in posterior disc height at the L3/4.

Pearcy and Tibrewal et al. [24] investigated the ranges of lateral bending plus the accompanying rotations in the planes other than that of the primary voluntary movements in two groups of normal male volunteers using a three-dimensional radiographic technique. They reported larger bending ranges in the upper segments when compared with the lower levels of the vertebrae, which was basically in line with our results. However, Li et al. [20] found that the L4-5 had a larger range of left-right bending motion than the L3-4. In their study, an unrestricted lateral bending was performed by all subjects, which is different from our restriction on the position of the pelvis and hips to a certain extent. The differences between the data emphasize the importance of motion patterns when investigating vertebral kinematics.

Finite element studies have also simulated the biomechanical responses of the disc. Wang et al.[5] created three 3D finite element models of the L3-4 disc using MR images. During the weight lifting extension, the L3-4 disc experienced a maximum shear load of about 230 N or 0.34 bodyweight at the flexion position and the maximum compressive load of 1500 N or 2.28 bodyweight at the upright position. Masni-Azian et al. [18] created a three-dimensional nonlinear finite element model of the L4-L5 functional spinal unit. At a moment of 10 Nm and compression of 500 N, the degenerated IVD obtained the maximum shear strain in the posterolateral area during lateral bending. Wu et al. [25] investigated *in vivo* motion of the lumbar spine during a weight-lifting activity. Their data showed that the lower lumbar motion segments L4/5 had larger anterior-posterior and proximal-distal translations than the upper lumbar segments. Considering the magnitude of compression load in different experiments,[26] it explained that small load (10kg) had no significant effect on disc deformation. Moreover, our subjects were mainly lower lumbar discs of young asymptomatic patients.

To our knowledge, few previous studies have reported data on the geometric deformation of the lumbar intervertebral disc during lateral bending. Most of the researches concentrate on the changes of lumbar segments during flexion and extension and the coupled motion patterns. Wang et al. [9] measured the geometric deformation of lumbar intervertebral discs under in-vivo weightbearing conditions using DRIS. The average maximum tensile deformation was − 21% in compression and 24% in tension, and maximum shear deformation on the disc surface reached 26%. In general, the higher-level discs have higher deformation values. To sustain body weight during standing, lumbar lordosis increases which causes the anterior location of the L3-4 disc to be under tension and the posterior location to be under compression. To balance the tension of the L3-4 (left-anterior tension, right-posterior tension), the left portion of the L4-5 was compressed and the right portion was tensed. The movement patterns during lateral bending can be explained by physiological weightbearing conditions. From the supine to the standing, and then to the bending, the combination of weight and posture causes the diagonal deformation of the lumbar disc, in which the measured tensile deformation of the L3-4 and L4-5 discs range from 15% to -40%, and the shear strain range is rather constant from 30–60% during maximum lateral bending.

Although most of the subjects showed similar patterns of disc deformation, despite our efforts to standardize the experiment, differences between subjects can still be expected and observed. We found that the direction of some disc deformation is opposite to the direction of motion. When considering possible, to maintain postural stability, the vertebral body performs compensatory motion. This may be related to the phenomenon of compensatory scoliosis. [8, 24, 27, 28] In the future, we plan to increase the number of test subjects in order to improve statistical ability, discover more different movement patterns, and conduct statistical induction.

The present study has several limitations. First of all, the sample size is too small, which limits our ability to observe the differences in motion patterns. It also explains why some of the differences found are not statistically significant, and the large SD obtained. Although we revealed the difference in the changes in disc deformation during lateral bending motion under different load-bearing conditions, we could not analyze the effects of age and gender on vertebral kinematics. Also, the assistance provided to exercise is not sufficient. In order to complete the maximum side bending and maintain the posture, the body may need exercise compensation and cannot complete the typical and standardized exercise form. Hence, due to the size limitation of the fluoroscope, we only examined the end-of-motion status of the segment L3-5, which has a high probability of degenerative lumbar disease. We did not check the instantaneous position of the human body during dynamic movement of the vertebral body. Future work should overcome these limitations. Despite these limitations, this study systematically examined the changes in disc deformation during lateral bending motion under different load-bearing conditions.

Conclusion

In summary, this study used DFIS to study functional lumbar motion in human subjects under physiological conditions. The advantage of this system for spine research is that it faithfully reproduces the in-vivo vertebral body motion model, taking into account the combined effects of various factors such as muscles and ligaments. This article reports data on the range of motion of the lumbar spine during different weight-bearing lateral bending exercises. We found that lumbar disc deformation showed direction-specific and level-specific changes during lateral bending motion. These data may provide new insights into the function of the human spine in vivo. Future research will focus on the use of 3D finite element analysis while using the kinematics data determined in this research as boundary conditions to examine the strain state of lumbar spine segments under pathological conditions.

Abbreviations

LDD: Lumbar Intervertebral Disc Degeneration

DFIS: dual fluoroscopic imaging system

6DOF: six degrees of freedom

FE: Finite element

Declarations

Ethics approval and consent to participate

The study protocol was approved by the local ethics committee (Tianjin Hospital Ethics Committee).

Consent for publication

Not applicable.

Availability of data and materials

Not applicable

Competing interests

The authors declare that they have no competing interests.

Funding

The research has received funding from the National Natural Science Foundation of China (grant no. 81472140) and Natural Science Foundation of Tianjin City (grant no. 20JCZDJC00800).

Authors' contributions

JM conceived and designed the study. WQW, ZPZ and BWK completed this experiment. JCW and HPX analyzed the data. HXX wrote the manuscript. All authors read and approved the final manuscript.

Acknowledgements

The financial support from the National Natural Science Foundation of China was greatly appreciated. This research was also supported by Department of Spine Surgery at Tianjin Hospital.

Author details

1 Clinical Department of Orthopaedics, Tianjin Medical University, 406 Jiefang South Road, Hexi District, Tianjin, China.

2 Spine Surgery, Tianjin Hospital, 406 Jiefang South Road, Hexi District, Tianjin, China.

Corresponding author: Jun Miao, MD, Department of Spine Surgery, Tianjin Hospital, Jiefangnanlu 406, Hexi District, Tianjin, China. 300210.Tel: +86-18920322787; Fax: +86-022-60910161; (E-mail: mj6688@163.com).

References

1. Byrne RM, Aiyangar AK, Zhang X. A Dynamic Radiographic Imaging Study of Lumbar Intervertebral Disc Morphometry and Deformation In Vivo. Sci Rep. 2019;9:15490.
2. Liu J, Hao L, Suyou L, Shan Z, Maiwulanjiang M, Li S, et al. Biomechanical properties of lumbar endplates and their correlation with MRI findings of lumbar degeneration. Journal of Biomechanics. 2016;49:586–93.
3. Liu J, Ebraheim NA, Haman SP, Shafiq Q, Karkare N, Biyani A, et al. Effect of the increase in the height of lumbar disc space on facet joint articulation area in sagittal plane. Spine. 2006;31:E198-202.
4. Wang S, Xia Q, Passias P, Li W, Wood K, Li G. How Does Lumbar Degenerative Disc Disease Affect the Disc Deformation at the Cephalic Levels In Vivo? Spine. 2011;36:E574–81.
5. Wang S, Park WM, Kim YH, Cha T, Wood K, Li G. In vivo loads in the lumbar L3-4 disc during a weight lifting extension. Clin Biomech (Bristol, Avon). 2014;29:155–60.
6. Berger-Roscher N, Casaroli G, Rasche V, Villa T, Galbusera F, Wilke H-J. Influence of Complex Loading Conditions on Intervertebral Disc Failure: Spine. 2017;42:E78–85.
7. Lidar Z, Behrbalk E, Regev GJ, Salame K, Keynan O, Schweiger C, et al. Intervertebral Disc Height Changes After Weight Reduction in Morbidly Obese Patients and Its Effect on Quality of Life and Radicular and Low Back Pain: Spine. 2012;37:1947–52.
8. Shin J-H, Wang S, Yao Q, Wood KB, Li G. Investigation of coupled bending of the lumbar spine during dynamic axial rotation of the body. Eur Spine J. 2013;22:2671–7.
9. Wang S, Xia Q, Passias P, Wood K, Li G. Measurement of geometric deformation of lumbar intervertebral discs under in-vivo weightbearing condition. Journal of Biomechanics. 2009;42:705–11.
10. Marini G, Huber G, Püschel K, Ferguson SJ. Nonlinear dynamics of the human lumbar intervertebral disc. Journal of Biomechanics. 2015;48:479–88.
11. Schmidt H, Häussler K, Wilke H-J, Wolfram U. Structural behavior of human lumbar intervertebral disc under direct shear. J Appl Biomater Funct Mater. 2015;13:66–71.

12. Amin DB, Lawless IM, Sommerfeld D, Stanley RM, Ding B, Costi JJ. The effect of six degree of freedom loading sequence on the in-vitro compressive properties of human lumbar spine segments. Journal of Biomechanics. 2016;49:3407–14.
13. Fu M, Ye Q, Jiang C, Qian L, Xu D, Wang Y, et al. The segment-dependent changes in lumbar intervertebral space height during flexion-extension motion. Bone & Joint Research. 2017;6:245–52.
14. Zhong W, Driscoll SJ, Wu M, Wang S, Liu Z, Cha TD, et al. In Vivo Morphological Features of Human Lumbar Discs. Medicine. 2014;93:e333.
15. Bennett CR, Kelly BP. Robotic application of a dynamic resultant force vector using real-time load-control: Simulation of an ideal follower load on Cadaveric L4–L5 segments. Journal of Biomechanics. 2013;46:2087–92.
16. Bisschop A, Kingma I, Bleys RLAW, Paul CPL, van der Veen AJ, van Royen BJ, et al. Effects of repetitive movement on range of motion and stiffness around the neutral orientation of the human lumbar spine. J Biomech. 2013;46:187–91.
17. Kuai S, Guan X, Li Y, Liu W, Xu Y, Zhou W. Influence of Deviated Centers of Rotation on Kinematics and Kinetics of a Lumbar Functional Spinal Unit: An In Vitro Study. Med Sci Monit. 2019;25:4751–8.
18. Masni-Azian, Tanaka M. Biomechanical investigation on the influence of the regional material degeneration of an intervertebral disc in a lower lumbar spinal unit: A finite element study. Computers in Biology and Medicine. 2018;98:26–38.
19. Wang S, Passias P, Li G, Li G, Wood K. Measurement of Vertebral Kinematics Using Noninvasive Image Matching Method–Validation and Application. Spine. 2008;33:E355.
20. Li G, Wang S, Passias P, Xia Q, Li G, Wood K. Segmental in vivo vertebral motion during functional human lumbar spine activities. Eur Spine J. 2009;18:1013–21.
21. Miao J, Wang S, Park WM, Xia Q, Fang X, Torriani MP, et al. Segmental spinal canal volume in patients with degenerative spondylolisthesis. Spine J. 2013;13:706–12.
22. Bai JQ, Hu YC, Du LQ, He JL, Liu K, Liu ZJ, et al. Assessing validation of dual fluoroscopic image matching method for measurement of in vivo spine kinematics. Chinese Medical Journal. 2011;124:1689–94.
23. Lichti DD, Sharma GB, Kuntze G, Mund B, Beveridge JE, Ronsky JL. Rigorous Geometric Self-Calibrating Bundle Adjustment for a Dual Fluoroscopic Imaging System. IEEE Transactions on Medical Imaging. 2015;34:589–98.
24. Pearcy MJ, Tibrewal SB. Axial rotation and lateral bending in the normal lumbar spine measured by three-dimensional radiography. Spine (Phila Pa 1976). 1984;9:582–7.
25. Wu M, Wang S, Driscoll SJ, Cha TD, Wood KB, Li G. Dynamic motion characteristics of the lower lumbar spine: implication to lumbar pathology and surgical treatment. Eur Spine J. 2014;23:2350–8.
26. Schmidt H, Shirazi-Adl A, Galbusera F, Wilke H-J. Response analysis of the lumbar spine during regular daily activities–a finite element analysis. J Biomech. 2010;43:1849–56.

27. Panjabi M, Yamamoto I, Oxland T, Crisco J. How does posture affect coupling in the lumbar spine? Spine (Phila Pa 1976). 1989;14:1002–11.
28. Barnes D, Stemper BD, Yoganan N, Baisden JL, Pintar FA. Normal coupling behavior between axial rotation and lateral bending in the lumbar spine - biomed 2009. Biomed Sci Instrum. 2009;45:131–6.

Figures

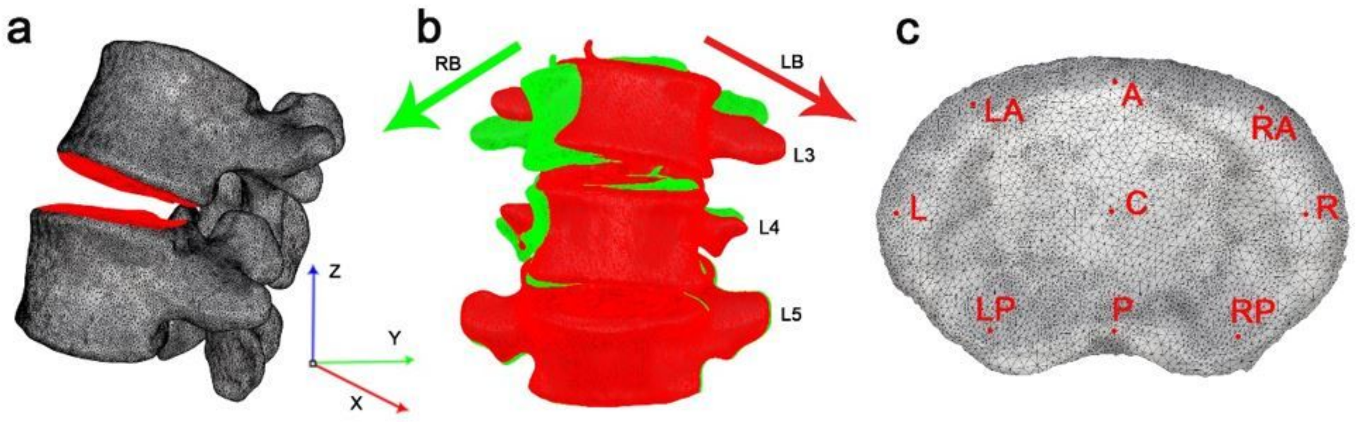

Figure 1

(a) 3D lumbar segmental model constructed from CT images, Upper and lower end plate; (b) Vertebral body position during left-right bending; (c)The representative locations on a disc surface: A—anterior, RA—right anterior, R—right, RP—right posterior, P—posterior, LP—left posterior, L—left, LA—left anterior and C-center.

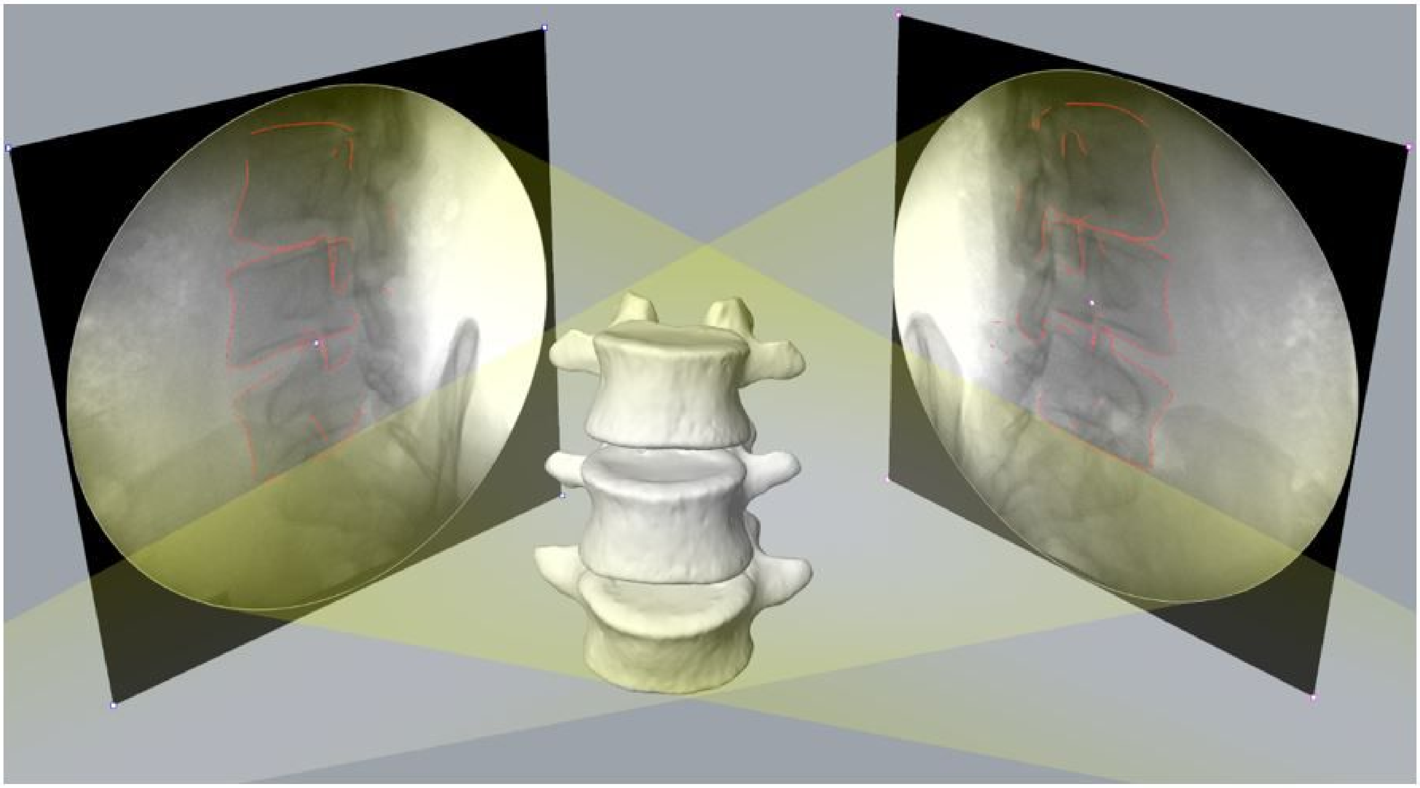

Figure 2

The virtual dual fluoroscopic system mimics the actual fluoroscopic system and was used to reproduce the in vivo vertebral positions

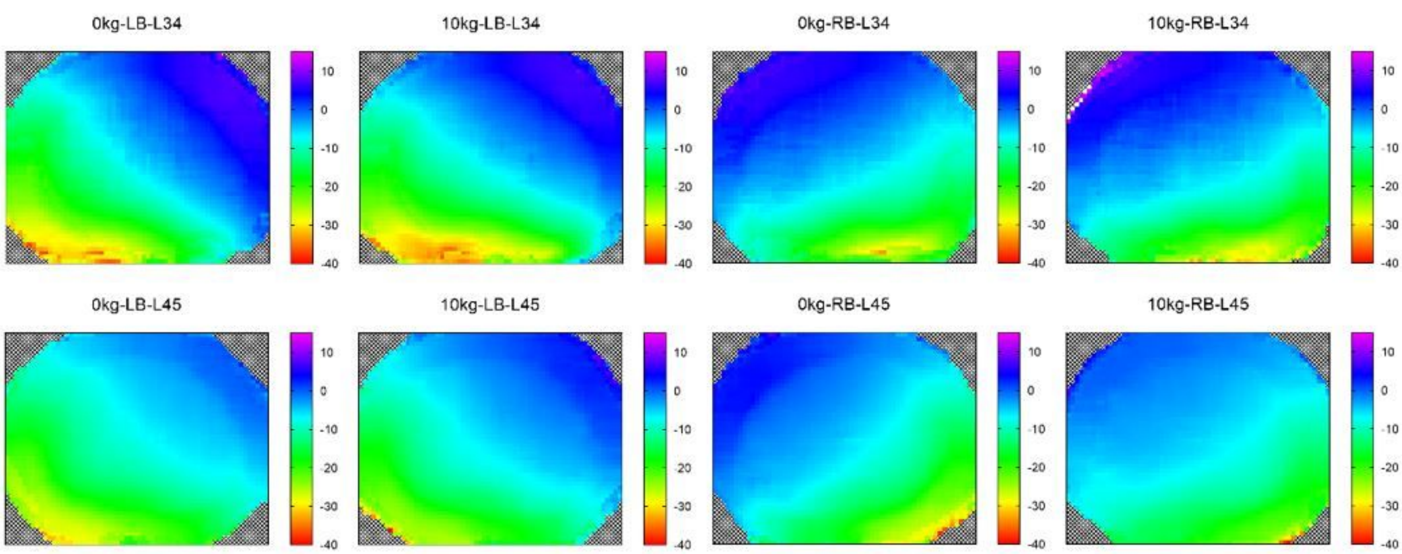

Figure 3

Weightbearing and 10Kg loading tensile deformation of the discs at different vertebral levels

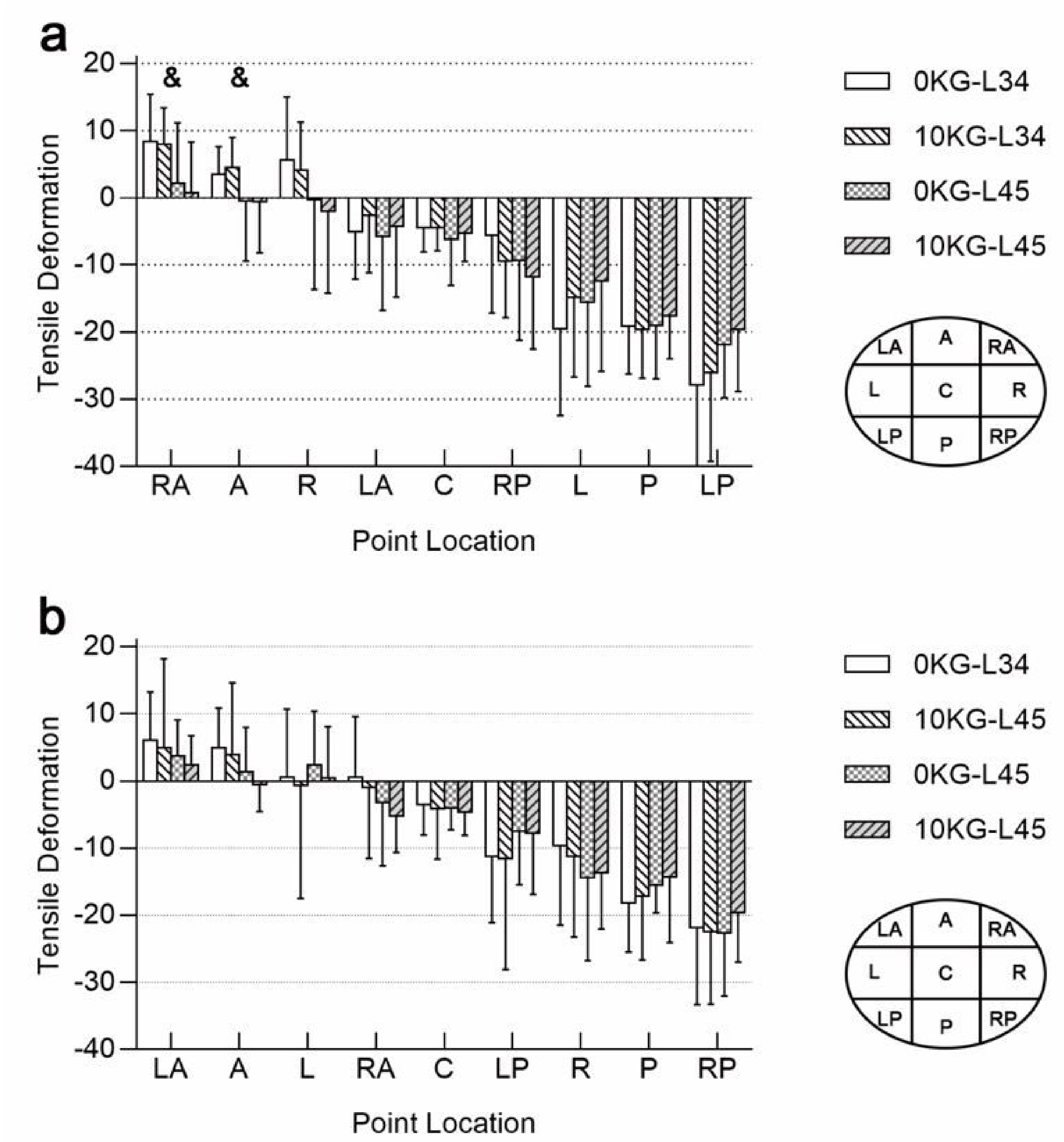

Figure 4

During (a) left bending and (b) right bending, tensile deformation at the 9 representative locations on disc surfaces with error bars showing the standard deviation; &: L3-4 different from L4-5, $p<0.05$.

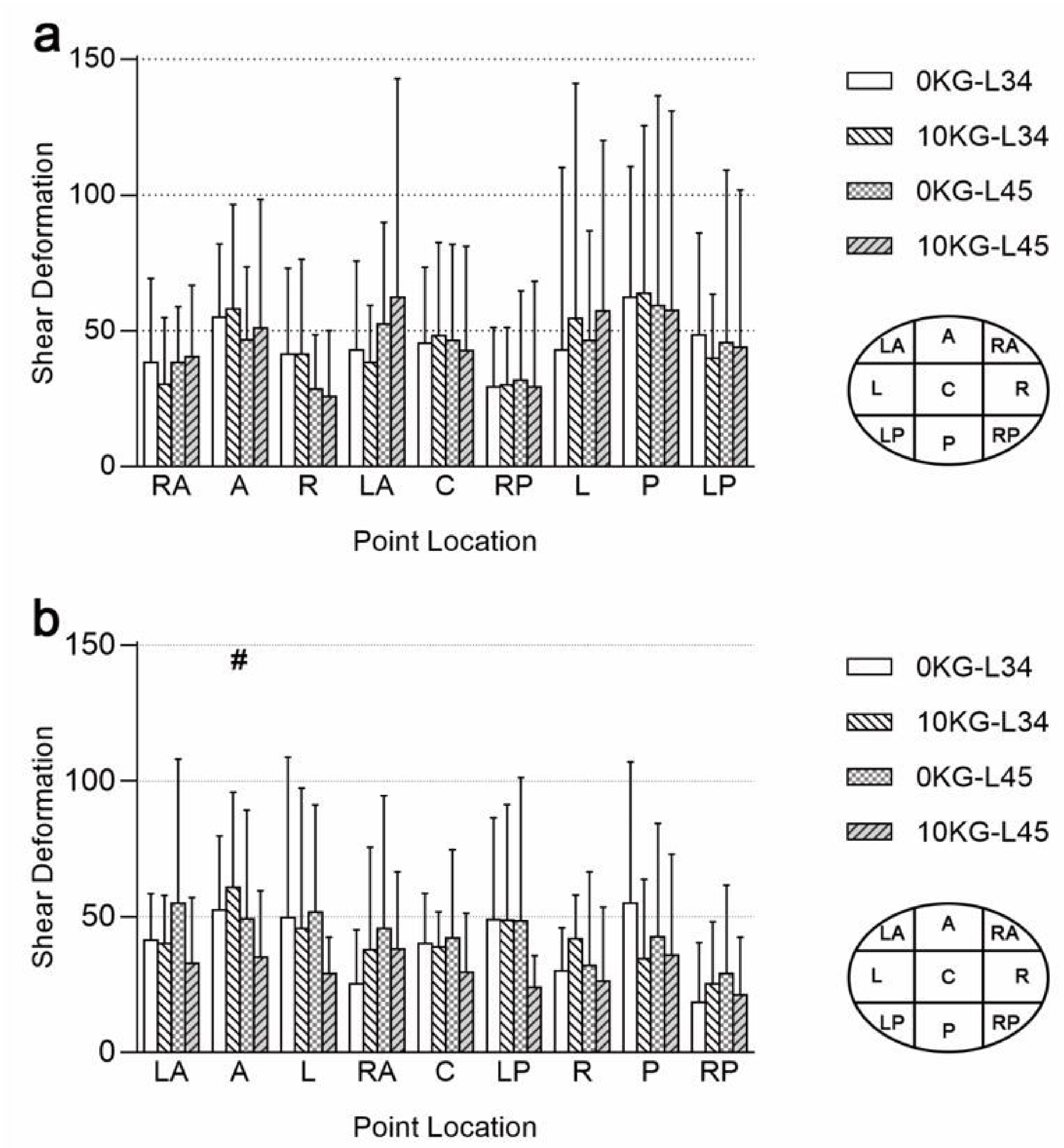

Figure 5

During (a) left bending and (b) right bending, shear deformation at the 9 representative locations on disc surfaces with error bars showing the standard deviation; #: L3-4 different from L4-5, p<0.05.